# Dye diazonium-modified carbon nanotubes with immobilized gold nanoparticles as nanohybrid electrocatalyst of direct methanol oxidation

Asma Bensghaïer[1*], Viplove Bhullar[2], Navdeep Kaur[2], Momath Lo[3], Myriam Bdiri[1], Aman Mahajan[2*], Mohamed M. Chehimi[1]*

[1] Université Paris Est, ICMPE (UMR7182), CNRS, UPEC, F-94320 Thiais, France
[2] Department of Physics, Guru Nanak Dev University, Amritsar-143005, Punjab, India
[3] Université Cheikh Anta Diop, Faculté des Sciences, BP 5005 Dakar-Fann, Senegal

**Abstract:** In a world of constant rush towards novel energy sources, hybrid nanomaterials have raised huge interest as their components can synergistically improve the expected performances in terms of power. In this regard, direct methanol oxidation (DMO) is among the most investigated reactions for implementation in portable and other devices. Herein, we report the design of gold-decorated CNT-aryl nanohybrids as electrocatalyst of DMO. In a first step, Azure A (AA), Neutral Red (NR) and Congo Red (CR) dye diazonium salts were reacted with CNTs to provide CNT-Dye nanoscale platforms for the immobilization of gold NPs. This step was conducted with CNT-Dye platforms evenly spread over glassy carbon (GC) electrodes. The CNT-Dye@Au nanohybrid electrode materials served for DMO electrocatalysis. Cyclic voltammograms show that bare CNT-Dye nanohybrids exhibit high electrocatalytic activity, particularly for the CNT-CR nanohybrid which returned a 3-fold improvement. With anchored Au NPs, a further 4 time remarkable increase in the oxidation peak intensity was achieved (*i.e.* about 12-fold the peak intensity recorded in the absence of any nanocatalyst). The forward to the backward anodic peak current density ratio $J_f/J_b$ was found to be as high as is 1.68.

This work provides a simple, elegant and efficient approach for designing robust, nanohybrid electrocatalyst for DMO, based on the smart combination of CNTs, diazotized dyes and gold NPs.

**Keywords:** diazonium salts; dyes; multiwalled carbon nanotubes; gold nanoparticles; direct methanol oxidation; electrocatalysts.

**Decalaration of interest:** the authors declare no conflict of interest

**Corresponding authors:**
A. Bensghaïer: asmabensghaier18@yahoo.com
M. M. Chehimi: chehimi@icmpe.cnrs.fr , **ORCID:** 0000-0002-6098-983X
A. Mahajan**:** aman.phy@gndu.ac.in

## 1. Introduction:

Fuel cells convert the energy stored in chemicals into electricity without burning, therefore avoiding the inefficiency of the polluting process such as traditional combustion. The growing interest in fuel cells is indeed testified by number of publications indexed in Web of Science since the early 21st century.‡ Direct methanol fuel cells (DMFCs) are considered to be one of the most attractive portable power sources due to their environment friendly nature, simplicity, and high durability [1,2]. The performance of DMFCs highly depends upon the charge transportation processes. In order to enhance the transportation of charge throughout this electrochemical device, a support system such as an electrocatalyst is required. An electrocatalyst should be electrically conductive and resistant to corrosion in an electrochemical environment. The most active anode materials explored for methanol oxidation reactions (MOR) are nanostructured platinum (Pt) and its alloys owing to their large surface area which provides more active sites, thus leading to high energy conversion efficiency [3,4]. However, high cost, lack of resources and poisoning of active sites of Pt electrocatalyst by residual carbon monoxide (CO) in MOR limits the widespread commercialization of the DMFCs [5,6]. To design an efficient and environmental friendly catalyst for DMFCs is a challenging task. It rests on the choice of metallic nanocatalyst among other parameters. In this regard, Au, Ag, Pd and Rh metallic nanoparticles are suitable substitutes for Pt. They exhibit an excellent catalytic activity in oxidation reduction reactions (ORR) and interestingly they show higher stability during MOR against CO poisoning intermediate [6,7,8,9,10]. However, these metallic nanoparticles can only be efficient if they are in the solid state, dispersed media. In this regard, carbon nanomaterials emerged as versatile platforms for the dispersion of nano-electrocatalysts [11,12,13,14]. Carbon nanotubes (CNTs) were explored for proton exchange membranes and as catalyst support in fuel cells [15,16,17,18] and for biofuel cells as anode materials [19]. CNT covalent surface modification is mandatory in order to build stable supporting material that can resist to high temperature and ultrasonication. Carbon covalent functionalization could be achieved through chemical or electrochemical routes; such as oxidation, esterification, amidation or diazotization [20,21]. Diazonium surface chemistry is an easy and effective mean for the modification of CNTs. This could be achieved with either isolated or in situ generated diazonium salts from aromatic amine precursors with a result of covalently attached

‡ The topic "fuel cell" returns 1,500-7,600+ papers a year from 2001 to 2010 and 8,500-12,000+ papers indexed in Web of Science (data for year 2020 is partial). Last accessed 29 July 2020.

nanometer scale aryl layer. Of utmost importance, the said layer has uniform thickness and withstands heat and (sono)chemical treatments. This plays an important role for enhancing the electrocatalytic activity by creating strong substrate for metal NPs deposition [11,22].

Dyes have numerous functions besides staining textiles or biological cells; however the recent decades have witnessed their implementation in electronic devices such as chemiresistive gas sensors [23,24,25], fuel cells [26,27]. Azure A dye was used for electrocatalytic application such as the oxidation of NADH [28]. Azo dyes were used for microbial fuel cell [29]. Congo Red azo dye is widely used as a pH indicator [pH variation between 3-5 (from blue to red)]. Neutral red was investigated for pH measurement as an optode material [30], and as demonstrated by some of us, CNT-NR hybrid exhibit excellent pH responsive behavior [31].

Given the heterocyclic nature of the dyes grafted to CNTs and the remarkable properties they impart to the latter, we reasoned that such aryl would be beneficial for the immobilization of metallic nanocatalysts such as gold nanoparticles. Much has been said about the attachment of nanocatalysts to aryl-modified CNTs [11] and other carbon allotropes [32], but the process concerned only classical functional groups borne by the phenyl rings from the aryl layer, namely $NH_2$, SH, COOH. For this reason, this works offers alternative anchoring groups from dye diazonium salts for nanocatlysts. This choice was motivated by the rich chemical composition of the dyes providing azo groups and phenothiazine blocks.

Herein, we propose a new and efficient process of using CNT-Dye nanohybrids for the DMFC application and to extend it to applied aspects. For synthesizing CNT-Dye nanohybrids, we took advantage of a synthesis protocol conducted in water at RT [31] in order to synthesize robust CNT-Dyes nanohybrids namely; CNT-AA, CNT-NR and CNT-CR. A comparative study of the catalytic efficiency of CNT-Dye and CNT-Dye@Au nanoparticles was performed as well. The grafted aromatic heterocyclic compounds could easily bind gold nanoparticles (Au NPs). Despite the developments in surface chemistry, nanomaterials and energy sources summarized above, no similar nanohybrids were reported before, that combine the salient properties of CNTs, dyes and Au NPs for the purpose of new energy sources.

## 2. Experimental

### 2.1. Materials

Azure A, Neutral Red and Congo Red (all Alfa Aesar products) were used as received. MWCNTs (diameter 1–10 nm, length 60-100 nm, purity >90%) were Nanocyl 7000 products. Deonized water was used for various cleaning and dilution processes. Ether and acetone (Aldrich, spectrophotometric grade) were used as received. MWCNTs were Nanocyl® - 7000 type purchased from Nanocyl S.A., Belgium. The MWCNT characteristics are the following: 90% purity, metal oxide impurity of 10 %, the average diameter is around 9.5 nm, the average length is 1.5 μm, and surface area is 250-300 $m^2/g$ (supplier's data). Dimethyl formamide (DMF) was purchased from Sigma Aldrich and used as the solvent for dispersion of CNT-Dye nanohybrids, Nafion® 117 solution (Sigma Aldrich) was used as proton conductor for proton exchange membranes (PEM). KOH solution as electrolyte for electrochemical measurements (Sigma Aldrich), tetrachloroauric acid ($AuHCl_4$) and sodium tricitrate ($C_{18}H_{15}Na_9O_{21}$) were purchased from Sigma Aldrich to synthesize the Au NPs.

### 2.2. Preparation of Au-decorated CNT-Dye nanohybrids

- Synthesis of CNT-Dye nanohybrids:

To prepare CNT-Dye (CNT-AA, CNT-CR and CNT-NR) nanohybrids, we adopted the same procedure previously reported by our team [31]. In short, 40 mg CNTs were modified in 200 ml water at RT with diazonium salts (200 mg) of Congo Red, Azure A and Neutral Red dyes named as; CR-$N_2^+$, AA-$N_2^+$, and NR-$N_2^+$, respectively.

- Deposition of Au NPs on CNT-CR nanohybrid:

Gold nanoparticles were prepared as previously described [33], using 0.5 M $AuHCl_4$, and $C_{18}H_{15}Na_9O_{21}$ solutions (0.5 M) [33]. The freshly prepared red wine colloidal solution was characterized using UV-visible method (Supplementary Material Fig. **SM1**) to track the absorption band located at 538 nm, a characteristic of Au NPs [34]. Meanwhile, the synthesized nanohybrids were gently dispersed in DMF for 15 min. at RT. After ultrasonication one can observe a homogenous dispersion, like ink. The as-prepared nanohybrid inks were drop-cast on pre-cleaned glassy carbon (GC) electrode. The deposited films were dried under air atmosphere for 1 h. To prepare CNT-CR@Au electrode, we drop-casted a thin layer of Au NPs solution on top of CNT-CR modified GC electrode dried film (prepared as previously described above). The deposited amount of Au NPs was left to dry under air atmosphere. Finally, 10 μL of Nafion® 117 solution was drop-cast on all prepared

electrodes. Nafion is a synthetic polymer used to ensure the attachment of CNT-Dye solutions and Au NPs solution to GC electrode; we noticed no leaching of the nanohybrids during the course of electrocalysis. During the electrocatalytic studies all measurements were carried out at RT in 0.5 M KOH solution.

### 2.3. Characterization of nanohybrids

X-ray diffraction (XRD) study was performed on D8 FOCUS, Bruker Ettlingen using Cu $K_\alpha$ line ($\lambda$ = 1.54 Å) in the range of 5–80˚. The morphology of nanohybrids was studied using Carl Zeiss (Supra 55) field emission scanning electron microscope (FESEM) fitted with an X-ray detector for the energy dispersive X ray spectroscopy (EDX). For investigating the optical properties of the samples, absorption spectra were recorded by using Shimadzu UV-2450 spectrophotometer. XPS spectra were recorded using K Alpha (Thermo) fitted with a monochromatic Al $K_\alpha$ X-ray source (spot size: 400 µm). The pass energy was set to 200 and 50 eV for the survey and the narrow regions, respectively. Electron and argon flood guns were used to compensate for the static charge build-up of the glassy carbon modified with Au nanoparticles. The composition was determined using the manufacturer sensitivity factors. The electrochemical measurement was performed using Autolab potentiostat galvanostat (PGSTAT302). A standard three compartments electrochemical cell was used with glassy carbon (GC) as anode, Pt wire as the counter electrode and saturated calomel electrode (SCE) as the reference electrode. Cyclic Voltammetry (CV) tests were carried out between -0.2 and 1.0 V at constant scan rates using PGSTAT302 system.

## 3. Results and Discussion

### 3.1. Modification of glassy carbon with CNT-Dye nanohybrid film

The CNT-Dye nanohybrids were prepared as previously reported [31]. CNT-Dye/GC and CNT-Dye@Au/GC electrocatalysts were studied for methanol oxidation reactions.

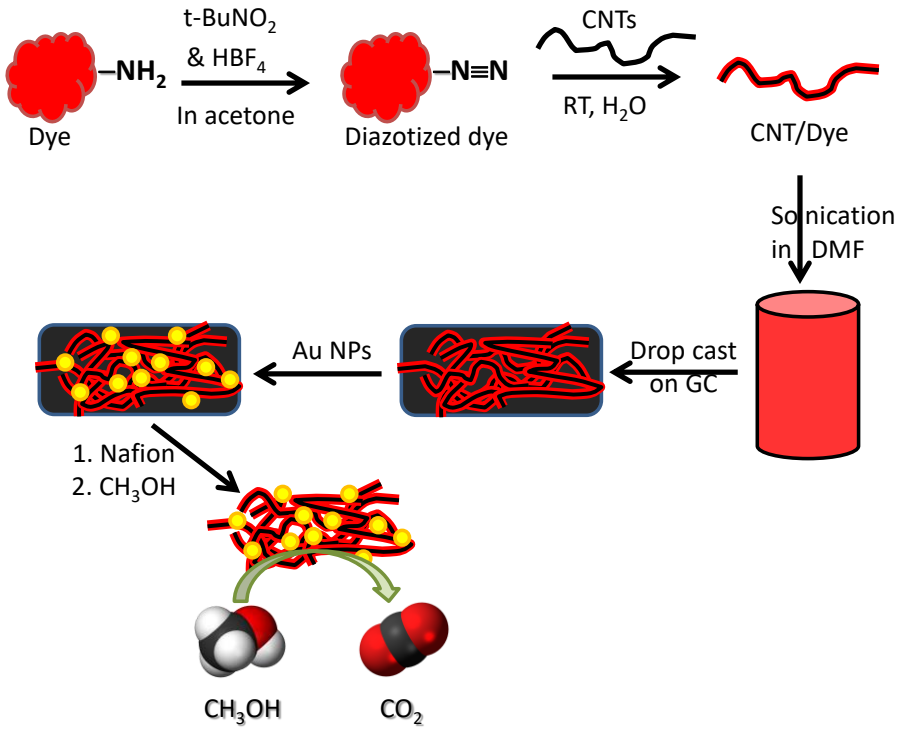


**Figure 1.** Upper panel: general pathway of dye diazonium synthesis and spontaneous aryl grafting of MWCNTs. Example is given for CR diazonium tetrafluoroborate. Lower panel: electrocatalyst fabrication for DMO measurements:
(1) CNT-Dye/GC, and (2) CNT-CR@Au/GC.

Fig. 1 (upper panel) describes a spontaneous pathway to prepare CNT-Dye nanohyrids by modifying CNTs with diazotized dyes in a simple and green process. The nanohybrids showed very good dispersions in DMF. As shown in the lower panel, the solution of CNT-Dye nanohybrid/DMF was drop casted onto GC electrode for MOR. Two routes were investigated for this purpose. Fig. 1 (1) shows GC electrode modified with CNT-Dye solution however, in fig. 1 (2) we drop casted Au NPs solution on CNT-CR/GC. We run a comparative study of the eletrocatalytic activity of the modified GC electrodes. DMO studies were done under same conditions (RT and in 0.5 M KOH solution).

### 3.2. X-ray powder diffraction analysis (XRD)

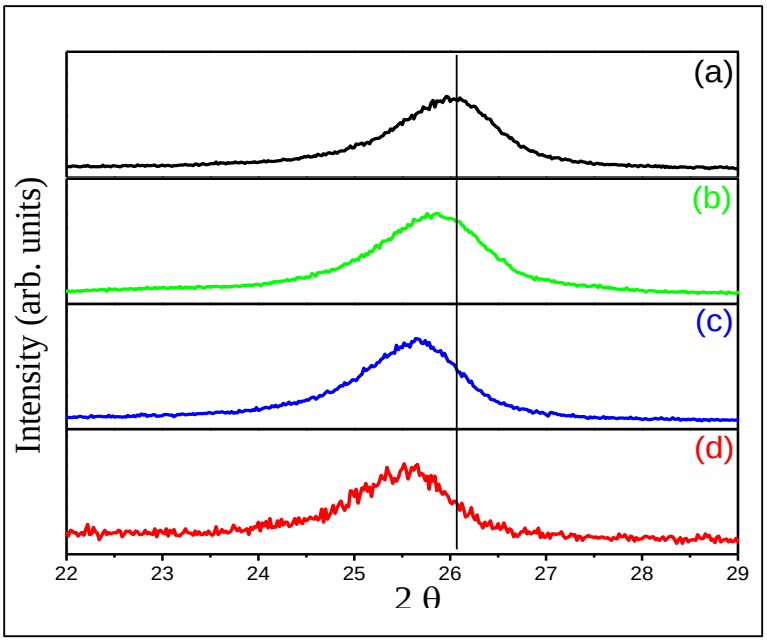


**Figure 2.** XRD patterns of (a) CNT, (b) CNT-$CR_{200}$, (c) CNT-$NR_{200}$, (d) CNT-$AA_{200}$. Diffraction peaks are indexed as C (JCPDS file no. 26-1076)..

Fig. 2 shows the XRD patterns of pristine and dye modified CNTs. The XRD pattern displayed in SM2a exhibit various diffraction peaks accounting for the crystalline hexagonal structure of carbon as referenced in (JCPDS 26-1076) [35, 36]. The intense (006) peak located at 26° suggests dominant exposure of these planes in the sample [37, 38]. Interestingly, the main peak (006) as shown in SM2(a-d) is present in all XRD patterns of CNTs and CNT-Dye nanohybrids which indicate that the hexagonal structure of carbon nanomaterial is maintained after covalent surface modification with dyes. On other hand, the peak position corresponding to (006) planes shifts from 26° (CNT) to 25.8° (CNT-CR) to 25.6° (CNT-NR) to 25.5° (CNT-AA) respectively as shown in Fig. 2. This shift in peak position suggests the presence of strain in the modified CNT. This strain can be estimated using relation:

$$\textit{macrostrain (\%)} = (d_{hkl}-d_r)/d_r,$$

where $d_r$ and $d_{hkl}$ are the interplanar spacing of reference sample (CNT) and modified sample, respectively [39]. The interplanar spacing $d=\lambda/2\sin\theta$ was obtained from known values of $\lambda$=1.54Å and respective peak position for (006) planes.

**Table 1:** d-spacing and macrostrain values of CNT and CNT-Dye nanohybrids

| Sample | CNT | CNT-CR | CNT-NR | CNT-AA |
|---|---|---|---|---|
| d-spacing (Å) | 3.42 | 3.44 | 3.47 | 3.48 |
| Macrostrain (%) | - | 0.5 | 1.32 | 1.54 |

As noted from Table 1, the d-spacing and macrostrain values increase with the grafting of dyes onto CNT surfaces [40]. The d-values increase with addition of dyes and corresponding positive macrostrain values confirm the lattice elongation [41].

### 3.3. Scanning Electron Microscopy (SEM) and EDX spectroscopy

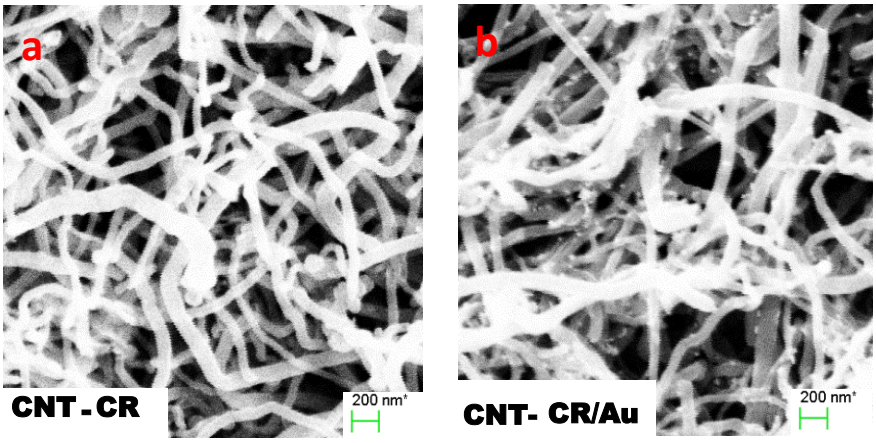


**Fig. 3.** SEM images of CNT-CR nanohybrid (a), and CNT-CR@Au NPs (b).

SEM was used to witness CNT surface modification with dye diazonium compounds by comparing their morphologies before and after grafting of dyes as shown in SM3. CNTs SEM image (SM3 (a)) shows more “dark holes” known as intertubular spaces as compared to CNT-Dyes nanohybrids (SM3b-d) [42]. Compared to the morphology of CNTs displayed in SM3a, the CNT-Dye hybrids imaged by SEM (see SM3b-d) exhibit neat texture, with smooth surface of the sidewalls. Fig. 3 shows SEM images of the analyzed CNT-CR versus CNT-CR@Au NPs. Clear morphological changes can be noted for the Au NPs treated sample; indeed numerous bright dots are uniformly distributed on the CNT-CR surface, interestingly without any agglomerated Au NPs (Fig. 3b)

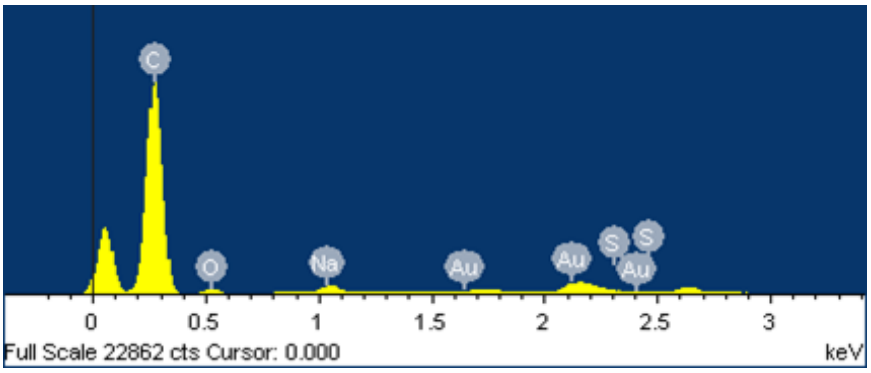


**Fig. 4.** EDX spectrum of CNT-CR@Au NPs.

To account for the change in the chemical composition of CNTs, we have analyzed the same nanotubes by EDX using the same SEM apparatus. The surface compositions are reported in **SM4**. Through EDX analysis, we were able to measure the elemental composition of each sample [43]. CNT is only composed of carbon atoms; CNT modified with dyes show C from CNTs and dyes molecules beside other elements. In case of CNT-AA we obtained nitrogen (N), oxygen (O), sulfur (S) and chloride (Cl), for CNT-NR the spectrum shows C, N and O whereas for CNT-CR; EDX shows C, N, O and S. Figure 4 displays EDX spectrum of CNT-CR@Au NPs and shows the effective impregnation of Au NPs onto CNT-CR platform. As sulfur is a unique elemental marker (from sulfonate groups in CR), $Au/SO_3$ atomic ratio was found to be 3, and thus Au/CR is 1.5 since CR has two sulfonate groups.

### 3.4. XPS

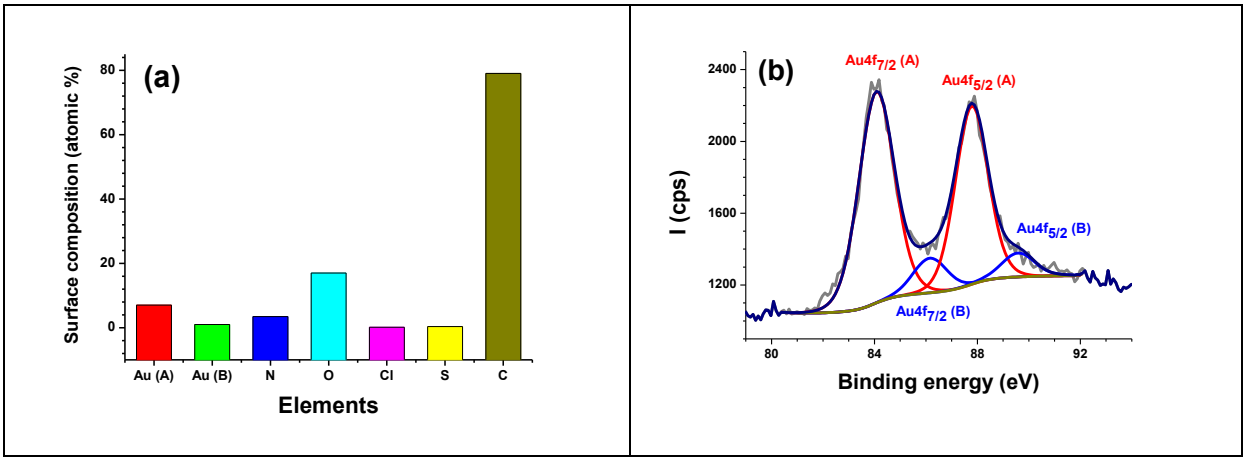


**Fig 5.** XPS analysis: surface composition (a), and high resolution Au4f spectrum of CNT-CR@Au NPs.

XPS was used to probe Au NPs deposited on CNT-CR/GC electrode. XPS survey region (**SM5)** shows C1s (285 eV), O1s (532 eV), N1s (400 eV) and S2p (168 eV) peaks from CR dye grafted onto CNTs [31], and Au4f doublet (84-88 eV) from the immobilized NPs. Interestingly, Fig. 5a exhibits two Au4f doublets with $Au4f_{7/2}$ core electron peaks located at 84 and 88 eV, respectively [40]. The peaks can be assigned to $Au^0$ and $Au^{+1}$ oxidation state of gold [44,45,46]. For each oxidation state, the $Au4f_{5/2}/Au4f_{7/2}$ intensity ratio is ~3/4 which is in line with theory. XPS permitted not only to confirm EDX results pertaining to Au NPs film deposition on CNT-CR nanohybrid, but also to bring strong supporting evidence for the major metallic state of Au. Fig. 5b exhibits the main peaks detected with different atomic% values relatively for CNT-CR nanohybrid atomic composition. The XPS determined atomic percent of Au reached 0.08% (including 0.07% for metallic Au). Therefore, the $Au/SO_3$ = 22.2 and Au/CR = 11.1; values way much higher than those obtained by EDX. This is in line with the more specific surface technique XPS which probe the outermost elements. In contrast, EDX is a more bulk technique probing up to 10 µm. Since the Au NPs are sitting on the CNT/CR hybrids, it is logical to obtain higher values by XPS compared to EDX for $Au/SO_3$ and Au/CR molar ratios.

### 3.5. CNT-Dye nanohybrids for methanol oxidation:

#### 3.5.1. CNT-Dye/GC

Cyclic voltammograms (CVs) for CNT-CR, CNT-NR, CNT-AA nanohybrids and commercial GC were recorded in 0.5 M KOH (electrolyte) and 0.5 M $CH_3OH$ solution at scan rate of 100 $mV.s^{-1}$. One can notice two peaks in the CV curves, first one is called forward anodic peak and it corresponds to oxidation of methanol, second one is called backward anodic peak and it corresponds to oxidation of left out species mostly CO [47]. The forward anodic peak current density ($J_f$) values for CNT-CR, CNT-NR and CNT-AA are 19.36, 10.9 and 12.4, respectively. Current density for CNT-CR is around 1.55 times than its value for GC electrode (12.5 mA $cm^{-2}$). The backward anodic peak current density ($J_b$) values of non-modified GC electrode, CNT-CR, CNT-NR and CNT-AA are 8.56, 9.42, 4.49 and 0.53 mA $cm^{-2}$, respectively.

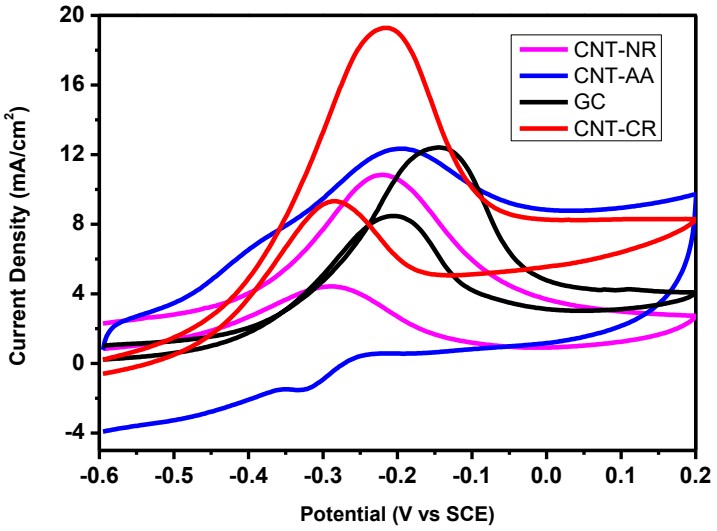


**Fig. 6.** Cyclic Voltammograms of CNT-NR, CNT-AA, GC and CNT-CR in 0.5 M KOH and 0.5 M $CH_3OH$ solution at scan rate of 100 mV $s^{-1}$.

Ratio of $J_f$ to $J_b$ i.e. $J_f/J_b$ is associated to the CO poisoning factor. Lower $J_b$ refers to a significant response for CO total oxidation during the forward scan. Thus a higher $J_f/J_b$ ratio is criterian for good electrocatalyst and lower $J_f/J_b$ ratio corresponds to poor oxidation of methanol in the forward scan [47, 13]. $J_f/J_b$ ratio for GC, CNT-CR, CNT-NR and CNT-AA are 1.46, 2.06, 2.42 and 23.39 as shown in Fig. 6. One can note that the CNT-Dye

nanohybrids have better anti-poisoning capability than GC electrode. However, $J_f/J_b$ ratio for CNT-AA seems to have the highest ratio among all used nanohybrids; the backward anodic peak for CNT-AA in Fig. 6 has unusual shape. This could explain the poor catalytic capability of CNT-AA to catalyze the left out species such as CO intermediate.

### 3.5.2. CNT-CR@AuNPs/GC

CNT-Dye are interesting materials for MOR however, CNT-CR nanohybrid shows best oxidation results according to CV voltamograms shown in Fig. 6. In the present work, we wished to go further and investigate more the possibility to enhance CNT-CR/GC electrode performances by immobilizing a pure well dispersed metallic nanoparticles, herein Au NPs. The Au NP dispersion was drop-cast onto the CNT-CR/GC electrode. Likely, the newly prepared CNT-CR@Au/GC electrocatalyst gives very high value of current density (55.11 mA $cm^{-2}$) towards MOR as compared to CNT-CR (19.36 mA $cm^{-2}$) [47].

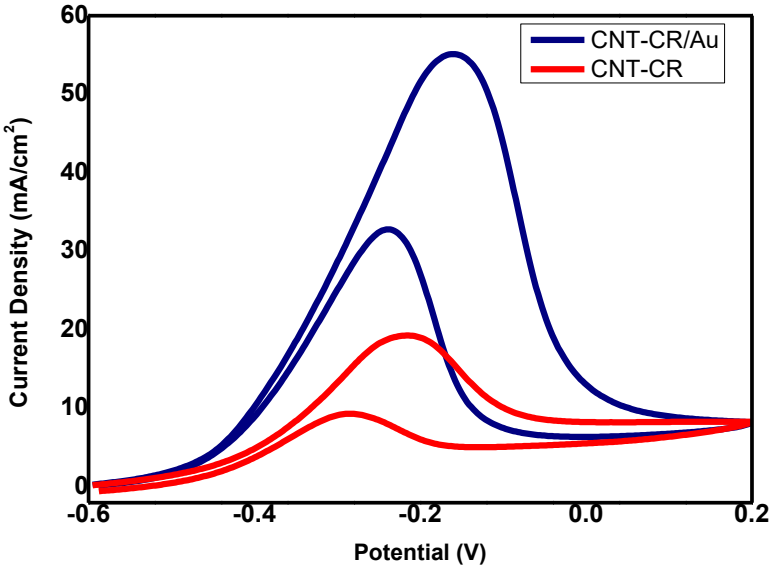


**Fig7.** Cyclic Voltammograms of CNT-CR and CNT-CR/Au in 0.5 M KOH and 0.5 M $CH_3OH$ solution at scan rate of 100 mV $s^{-1}$

The enhancement in the peak current density depicts the improved performance of CNT-CR@Au nanocatalyst in MOR by ~ 4 times compared to CNT-CR nanohybrid. According to literature, the results confirm that Au NPs are well dispersed with small size

particles onto CNT-CR surface otherwise they could not catalyze the methanol [48]. The oxidation potential for CNT-CR@Au of the oxidation peak is around -0.1 V compared to CNT-CR nanohybrid (-0.2 V), which represents a positive shift of 0.1 V in the oxidation potential as reported in Fig. 7. These results account for the electrocatalytic performances of the CNT-CR@Au nanocatalyst [49,50].

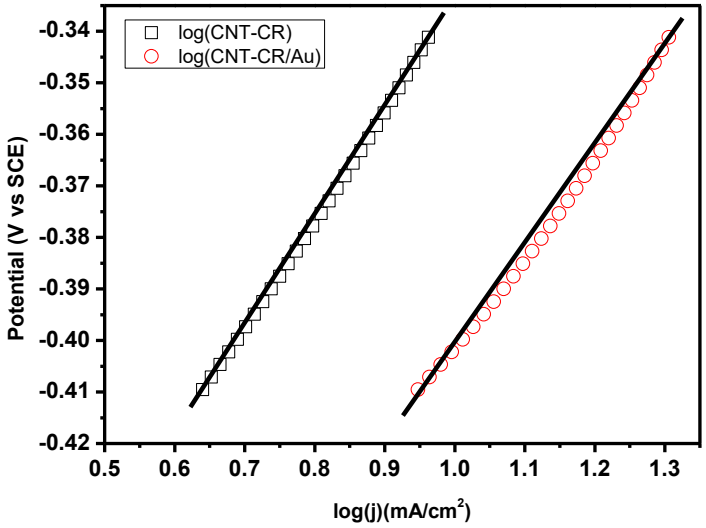


**Fig 8.** Tafel plots obtained from the rising portion of the forward anodic peak of CV curve on CNT-CR nanohybrid in 0.5 M KOH + 0.5 M methanol solution

Further, to evaluate the kinetic parameters (exchange current density and Tafel slope) associated with the catalytic activity of prepared electrocatalyst for MOR, the variation of electrode potential with the logarithm current density was investigated [13] (Fig. 8).

The exchange current density and Tafel slope for the cathodic process were evaluated using [51]:

$$\eta = a + b\,logj = -\frac{2.303RT}{\alpha nF}\log j_0 + \frac{2.303RT}{\alpha nF}\log j$$

where, $\eta$, $\alpha$, $F$, $T$, $R$, $j_0$ and $j$ refer to the over potential, charge transfer coefficient, Faraday's constant (96485.3 C/mol), absolute temperature, universal gas constant (8.314 J/mol K), exchange current density and apparent current density (in mA $cm^{-2}$), respectively. The constants $a$ and $b$ were found from the straight line fitting of variation of E-vs-log j. The

calculated exchange current corresponding to CNT-CR@Au and CNT-CR nanohybrids while catalyzing in methanol comes out to be 0.248 and 0.120 mA, respectively.

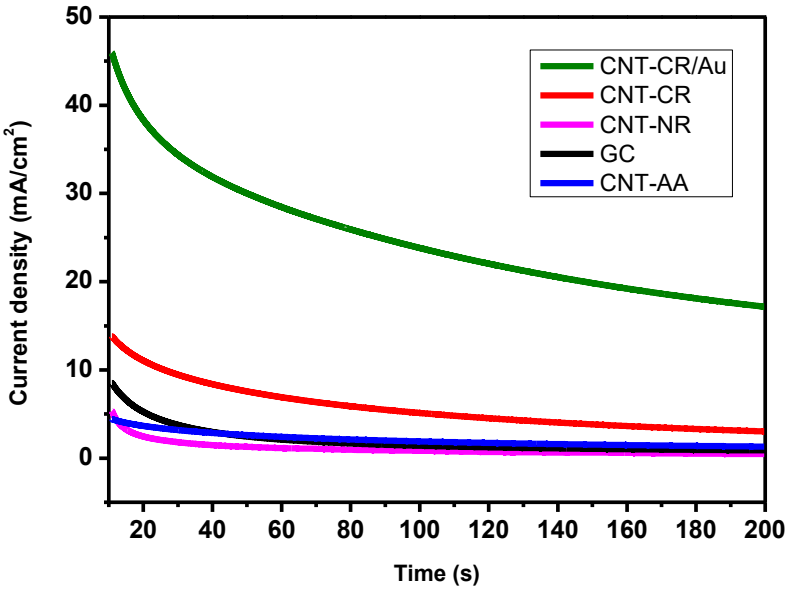


**Fig. 9.** Chronoamperometric measurements at -0.2 V for CNT-CR@Au/GC, CNT-CR/GC, CNT-NR/GC, GC electrode and CNT-AA/GC in 0.5 M KOH + 0.5 M $CH_3OH$ solution.

The durability of the electrocatalysts CNT-CR@Au, CNT-CR, CNT-NR, CNT-AA and bare GC, during long-term operation, was evaluated by chronoamperometric curves. Fig. 9 illustrates the current density (j)-vs-time (t) chronoamperometry which indicates that the CNT-CR@Au nanohybrid is more stable than all the other catalysts during long time operation.

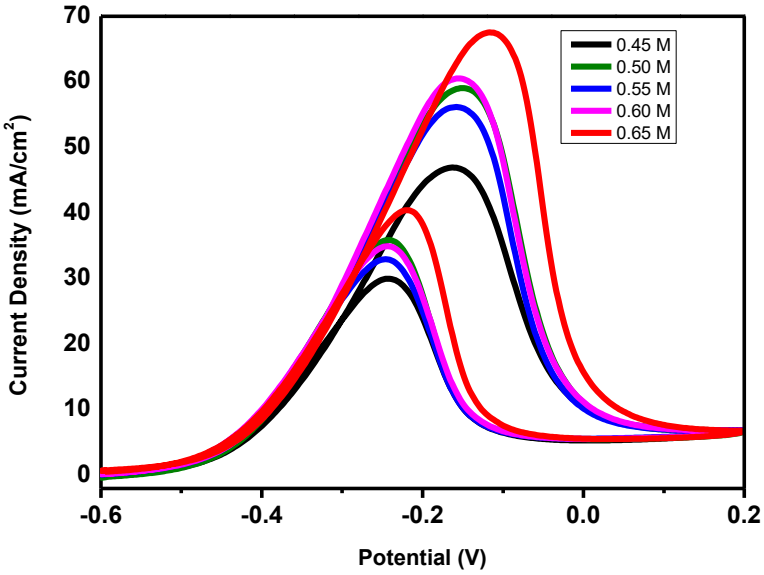


**Fig10.** CV curves of methanol oxidation with CNT-CR@Au/GC nanocatalyst in 0.5 M KOH solution with different methanol concentrations from (0.45-0.65 M)

Fig. 10 shows the CV curves of methanol oxidation using CNT-CR@Au catalyst with different methanol concentrations. The catalytic current density increases with the increase in methanol concentration. The increased methanol concentration accelerated the diffusion of methanol at the interface of catalysts and promotes the MOR process [52]. Thus, the above mentioned results demonstrate that the nanohybrid catalyst showed better performance for MOR [13] as compared to those reported in the literature (see Table 2).

**Table 2:** Summary of electrocatalytic studies on metal – CNT nanohybrids for DMO.

| S.No. | Material | $J_f/J_b$ | Reference |
|---|---|---|---|
| 1. | Pt nanoparticles on N-doped CNT | 1.15 | [53] |
| 2. | Pt on SWCNT | 0.94 | [54] |
| 3. | Pt on MWCNT | 1.65 | [55] |
| 4. | PdAu(Cu) on 3D rGO/CNT | 1.11 | [56] |
| 5. | alloy nanoparticles of Pt10_x–Fex supported on CNTs | 1.14 | [57] |
| 6. | Cerium Oxides on Pd/CNT | 1.38 | [58] |
| 7. | Pt and Pd on Au nanoparticles loaded CNT | 0.95 | [59] |
| 8. | Pt-Au/CNT@$TiO_2$ | 2.7 | [60] |
| 9. | CNT-CR@Au NPs | 1.68 | This work |

The $J_f/J_b$ ratio for CNT-CR@Au is ~1.68, higher than the values reported from the literature and gathered in Table 2, at the exception of Pt-Au/CNT@$TiO_2$ (entry 8). As our plan is to eliminate Pt-based electrodes or Pt nanoparticles for future fuel cells due to high cost issues, CNT-CR@Au NPs turn out to be an excellent alternative nanocatalyst for the electrocatalyzed DMO given its remarkable performances.

## Conclusion

In the domain of energy, the production of smart nanohybrid materials as electrocatalysts is ever growing and challenging. Herein, we contribute to this domain by designing CNT-CR@Au nanohybrids for the electrocatalyzed methanol oxidation reaction at the surface of GC electrodes. The CNT-Dye were prepared *via* diazonium chemistry and coated on GC prior to the even decoration by Au NPs. On one hand, the latter were found to be tightly attached to the diazonium-modified CNT sidewalls *via* electrostatic interactions, and synergetically improved the electrocatalytic properties of underlying nanotubes, on the other hand. These new nanohybrids not only impart superior electrocatalytic activity, enhanced current density and lower oxidation potential but also reduce the anti-poisoning (of e.g. Pt)

during methanol oxidation reaction process. These features of CNT-CR/Au nanohybrids make them favorable lower-cost candidates for direct methanol fuel cells than electrocatalysts based on Pt NPs. This opens new horizons for dye-modified CNTs ($sp^2$ nanocarbon allotropes in general) and their use as nanoplatform to construct new electronic devices (sensors, fuel cells, energy storage).

**Acknowledgements**
Authors acknowledge the department of Physics, GNDU, Amritsar, India for providing instrumentation. A. Bensghaïer is indebted to IFCEPAR/CEFIPRA for the provision of a Raman Charpak fellowship 2017 (N°IFC/ 4109/RCF 2017/874).

**References:**

[1] A.S. Aricò, S. Srinivasan, V. Antonucci. DMFCs: From Fundamental Aspects to Technology Development. Review, Fuel Cells 1 (2001) 133-161.

[2] W. Huang, H. Wang, J. Zhou, J. Wang, P.N. Duchesne, D. Muir, P. Zhang, N. Han, F. Zhao, M. Zeng, J. Zhong, C. Jin, Y. Li, S.-T. Lee, H. Dai. Highly active and durable methanol oxidation electrocatalyst based on the synergy of platinum–nickel hydroxide–graphene, Nat. Commun. 6 (2015) Art. No 10035.

[3] B. Dinesh, R. Saraswathi. Enhanced performance of Pt and Pt–Ru supported PEDOT–RGO nanocomposite towards methanol oxidation, Int. J. Hydrogen Energy 41 (2016) 13448-13458.

[4] W. Xie, F. Zhang, Z. Wang, M. Yang, J. Xia, R. Gui, Y. Xia. Facile preparation of PtPdPt/graphene nanocomposites with ultrahigh electrocatalytic performance for methanol oxidation, J. Electroanal. Chem. 761 (2016) 55-61.

[5] G. Singla, K. Singh, O.P. Pandey. Synthesis of carbon coated tungsten carbide nano powder using hexane as carbon source and its structural, thermal and electrocatalytic properties, Int. J. Hydrogen Energy 40 (2015) 5628-5637.

[6] M. Chatenet, L. Genies-Bultel, M. Aurousseau, R. Durand, F. Andolfatto. Oxygen reduction on silver catalysts in solutions containing various concentrations of sodium hydroxide – comparison with platinum, J. Appl. Electrochem. 32 (2002) 1131-1140.

[7] F. Shaik, W. Zhang, W. Niu, X. Lu. Volume-confined synthesis of ligand-free gold nanoparticles with tailored sizes for enhanced catalytic activity, Chem. Phys. Lett. 613 (2014) 95-99.

[8] K. G. Thomas, P. V. Kamat. Chromophore-Functionalized Gold Nanoparticles, Acc. Chem. Res. 36 (2003) 888-898

[9] P. Santhosh, A. Gopalan, K. P. Lee. Gold nanoparticles dispersed polyaniline grafted multiwall carbon nanotubes as newer electrocatalysts: Preparation and performances for methanol oxidation, J. Catalysis 238 (2006) 177-185.

[10] W.J. Long, R.M. Stroud, K.E. Swider-Lyons, D.R. Rolison. How To Make Electrocatalysts More Active for Direct Methanol Oxidation Avoid PtRu Bimetallic Alloys!, Phys. Chem. B 104 (2000) 9772–9776.

[11] D.J. Guo, H.L. Li. Highly dispersed Ag nanoparticles on functional MWNT surfaces for methanol oxidation in alkaline solution, Carbon 43 (2005) 1259–1264.

[12] J Luo, P.N. Njoki, Y Lin, D. Mott, L. Wang, C.J. Zhong. Characterization of carbon-supported AuPt nanoparticles for electrocatalytic methanol oxidation reaction, Langmuir 22 (2006) 2892-2898.

[13] S. Kumar, M. Mahajan, R. Singh, A. Mahajan. Silver nanoparticles anchored reduced graphene oxide for enhanced electrocatalytic activity towards methanol oxidation, Chem. Phys. Lett. 693 (2018) 23-27.

[14] Y. Guo, X. Sun, Y. Liu, W. Wang, H. Qiu, J. Gao. One pot preparation of reduced graphene oxide (RGO) or Au (Ag) nanoparticle-RGO hybrids using chitosan as a reducing and stabilizing agent and their use in methanol electrooxidation, Carbon 50 (2012) 2513-2523.

[15] G.L. Che, B.B. Lakshmi, C.R. Martin, E.R. Fisher. Metal-nanocluster filled carbon nanotubes: Catalytic properties and possible applications in electrochemical energy storage and production, Langmuir 15 (1999) 750–8.

[15] W.Z. Li, C.H. Liang, J.S. Qiu, W.J. Zhou, H.M. Han, Z.B. Wei, et al. Carbon nanotubes as support for cathode catalyst of a direct methanol fuel cell, Carbon, 40 (2002) 791–4.

[16] Z.L. Liu, X.H. Lin, J.Y. Lee, W. Zhang, M. Han, L.M. Gan. Preparation and characterization of platinum-based electrocatalysts on multiwalled carbon nanotubes for proton exchange membrane fuel cells, Langmuir 18 (2001) 4054–60.

[17]B. Rajesh, V. Karthik, S. Karthikeyan, K.R. Thampi, J.M. Bonard, B. Viswanathan. Pt–$WO_3$ supported on carbon nanotubes as possible anodes for direct methanol fuel cells, Fuel 81 (2002) 2177–90.

[18] Y. Qiao, C.M. Li, S.J. Bao, Q.L. Bao. Carbon nanotube/polyaniline composite as anode material for microbial fuel cells, J. Power Sources 170 (2007) 79-84.

[19] G.G. Wildgoose, C.E. Banks, R.G. Compton. Metal Nanoparticles and Related Materials Supported on Carbon Nanotubes: Methods and Applications, Small (2006). 2 (2006) 182-193.
[20] D. Tasis, N. Tagmatarchis, A.Bianco, M. Prato. Chemistry of carbon nanotubes, Chem. Rev. 106 (2006) 1105-1136.
[21] A. Bensghaïer, F. Mousli, A. Lamouri et al. The Molecular and Macromolecular Level of Carbon Nanotube Modification via Diazonium Chemistry: Emphasis on the 2010s Years, Chem. Africa (2020). https://doi.org/10.1007/s42250-020-00144-5
[22] P. Singh, S. Campidelli, S. Giordani, D. Bonifazi, A. Bianco, M. Prato. Organic functionalisation and characterisation of single-walled carbon nanotubes, Chem. Soc. Rev. 38 (2009) 2214–2230.
[23] A. Bensghaïer, N. Kaur, N. Fourati, C. Zerrouki, A. Lamouri, M. Beji, A. Mahajan, M.M. Chehimi. Diazonium chemistry for making highly selective and sensitive CNT-Neutral Red hybrid-based chemiresistive acetone sensors, Vacuum 155 (2018) 656-661.
[24] H. Banimuslem, A. Hassan, T. Basova, A. A. Esenpinar, S. Tuncel, M. Durmus, A.G. Gurek, V. Ahsen. Dye modified carbon nanotubes for the optical detection of amines vapors, Sens. Actuators, B 207 (2015) 224−234.
[25] A. Bensghaïer, K. Forro, M. Seydou, A. Lamouri, M. Mičušik, M. Omastová, M. Beji, M.M. Chehimi. Dye diazonium-modified multiwalled carbon nanotubes: light harvesters for elastomeric optothermal actuators, Vacuum 155 (2018) 178-184.
[26] MP Gore, LC Mann. Dye-based fuel indicator system.US Patent (2006). US 6,998,185 B2.
[27] S.D. Roller, H.P. Bennetto, G.M. Delaney, J.R. Mason, J.L. Stirling, C.F. Thurston Electron-transfer coupling in microbial fuel cells: 1. comparison of redox-mediator reduction rates and respiratory rates of bacteria, J. Chem. Technol. Biotechnol. 34 (1984) 13-27.
[28] C. Gomez-Anquela, M. Revenga-Parra, J.M. Abada, A. García´ Marín, J.L. Pau, F. Pariente, J. Piqueras, E. Lorenzo. Electrografting of N′,N′-dimethylphenothiazin-5-ium-3,7-diamine (Azure A) diazonium salt forming electrocatalytic organic films on gold or graphene oxide gold hybrid electrodes, Electrochim. Acta 116 (2014) 59−68.
[29] K. Solanki, S. Subramanian, S. Basu. Microbial fuel cells for azo dye treatment with electricity generation: A review, Bioresource Technology 131 (2013) 564-571.
[30] M. Fages. Study of the covalent grafting of dyes for the design of an optode for pH measurement, PhD Thesis, Université Paris-Saclay, France (2015).

[31] A. Bensghaïer, S. Lau Truong, M. Seydou, A. Lamouri, E. Leroy, M. Mičušik, K. Forro, M. Beji, J. Pinson, M. Omastová, M.M. Chehimi. Efficient covalent modification of multiwalled carbon nanotubes with diazotized dyes in water at room temperature, Langmuir 33 (2017) 6677−6690.

[32] P. Mirzaei, S. Bastide, A. Aghajani, J. Bourgon, E. Leroy, Ju. Zhang, Y. Snoussi, A. Bensghaïer et al. Bimetallic Cu-Rh nanoparticles on diazonium-modified carbon powders for the electrocatalytic reduction of nitrates, Langmuir 35 (2019) 14428-14436.

[33] O. Seitz, M.M. Chehimi, E. Cabet-Deliry, S. Truong, N. Felidj, C. Perruchot, S. J. Greaves, J. F. Watts, Colloids and Surfaces A 218 (2003) 225-239.

[34] H.N. Verma, P. Singh, R.M. Chavan. Gold nanoparticle: synthesis and characterization. Veterinary World, EISSN: 2231-0916.

[35] S. Cahen, G. Furdin, J.F.Marêche, A. Albiniak, Synthesis and characterization of carbon-supported nanoparticles for catalytic applications, Carbon 46 (2008) 511-517.

[36] B. Zhang, J.Wan, Waste Utilization Method for δ-MnO2 Anode Composited with MWCNT and Graphene by Embedding on Conductive Paper for Lithium-Ion Battery, Nano. 14 (2019) Art No 1950051, doi.org/10.1142/S1793292019500516

[37] V. Selen, Ö. Güler, D. Özer, E. Evin. Synthesized multi-walled carbon nanotubes as a potential adsorbent for the removal of methylene blue dye: kinetics, isotherms, and thermodynamics, Desalination and water treatment 57 (2015) 1-13.

[38] Investigating of a wide range of concentrations of multi-walled carbon nanotubes on germination and growth of castor seeds (Ricinus communis L.), J. Plant Protection Res. 57 (2017) 228-236.

[39] S. Sumithra. V. Jaya. Synthesis, Structural, Optical and Magnetic Properties of Pure NiO and NiO@$SiO_2$ Core–Shell Nanospheres, J. Supercond. Nov. Magn. 30 (2017) 1129–1136

[40] K. Jlassi, S. Zavahir, P. Kasak, I. Krupa, A. A. Mohamed, M. M. Chehimi. Emerging clay-aryl-gold nanohybrids for efficient electrocatalytic proton reduction. Energy Convers. Manag.168 (2018) 170-177.

[41] X.H.Yan. T.S.Zhao. L.An. G.Zhao. L.Shi. A direct methanol–hydrogen peroxide fuel cell with a Prussian Blue cathode, Int. J. Hydrogen Energy 41 (2016) 5135-5140.

[42] Dan-Dan Zhao, Zhi Yang, Eric Siu-Wai Kong, Cai-Ling Xu, Ya-Fei Zhang. Carbon nanotube arrays supported manganese oxide and its application in electrochemical capacitors, J. Solid State Electrochem. 15 (2011) 1235–1242.

[43] M.L. Chen, F.J.Zhang, W.C. Oh. Synthesis, characterization, and photocatalytic analysis of CNT/TiO2 composites derived from MWCNTs and titanium sources, New Carbon Mater. 24 (2009) 159–166.

[44] M. C. Bourg, A. Badia, R. B. Lennox. Gold-Sulfur Bonding in 2D and 3D Self-Assembled Monolayers: XPS Characterization, J. Phys. Chem. B. 104 (2000) 6562-6567.

[45]Y. Joseph, I. Besnard, M. Rosenberger, B. Guse, H. G. Nothofer, J. M. Wessels, U. Wild, A. Knop-Gericke, D. Su, R. Schlogl, A.Yasuda, T. Vossmeyer. Self-Assembled Gold Nanoparticle/Alkanedithiol Films: Preparation, Electron Microscopy, XPS-Analysis, Charge Transport, and Vapor-Sensing Properties, J. Phys. Chem. B 107 (2003) 7406-7413

[46] M. P. Casaletto, A. Longo, A. Martorana, A. Prestianni, A. M. Venezia. XPS study of supported gold catalysts: the role of Au0 and Au+δ species as active sites, Surf. Interface Anal. 38 (2006) 215–218.

[47] Y. Li, W. Gao, L. Ci, C. Wang, P.M. Ajayan. Catalytic performance of Pt nanoparticles on reduced graphene oxide for methanol electro-oxidation, Carbon 48 (2010) 1124–1130.

[48] J. Hernández, J. Solla-Gullón, E. Herrero, A. Aldaz, J.M. Feliu. Methanol oxidation on gold nanoparticles in alkaline media: Unusual electrocatalytic activity, Electrochim. Acta. 52 (2006) 1662-1669.

[49] Yu Shi, Ruizhi Yang, Pak K.Yuet. Easy decoration of carbon nanotubes with well dispersed gold nanoparticles and the use of the material as an electrocatalyst, Carbon 47 (2009) 1146 – 1151

[50] Z.J. Wang, M.Y. Li, Y.J. Zhang, J.H. Yuan, Y.F. Shen, L. Niu, et al. Thionine-interlinked multi-walled carbon nanotube/gold nanoparticle composites, Carbon 45 (2007) 2111–6.

[51] Y. Lin, X. Cui, C.H. Yen, C.M. Wai. PtRu/Carbon Nanotube Nanocomposite Synthesized in Supercritical Fluid: A Novel Electrocatalyst for Direct Methanol Fuel Cells, Langmuir 21 (2005) 11474-11479

[52] K.T. Jeng, C.C. Chien, N.Y. Hsu, S.C. Yen, S.D. Chiou, S.H. Lin, W.M. Huang. Performance of direct methanol fuel cell using carbon nanotube-supported Pt–Ru anode catalyst with controlled composition, J. Power Sources 160 (2006) 97–104.

[53] H.Y. Du, C.H. Wang, H.C. Hsu, U.S. Chen, S.C. Yen, L.C. Chen, H.C. Shih.Controlled platinum nanoparticles uniformly dispersed on nitrogen-doped carbon nanotubes for methanol oxidation, Diamond Relat. Mater. 17 (2008) 535-541

[54] A. Kongkanand, K. Vinodgopal, S. Kuwabata, P.V. Kamat. Highly Dispersed Pt Catalysts on Single-Walled Carbon Nanotubes and Their Role in Methanol Oxidation, J. Phys. Chem. B 110 (2006) 16185-16188.

[55] Y. Zhao L. Fan H. Zhong Y. Li S. Yang. Platinum Nanoparticle Clusters Immobilized on Multiwalled Carbon Nanotubes: Electrodeposition and Enhanced Electrocatalytic Activity for Methanol Oxidation, Adv. Funct. Mater. 17 (2007) 1537-1541.

[56] M. Wang, Z. Ma, R. Li, B. Tang, X.Q. Bao, Z. Zhang. Novel flower-like Pd Au (Cu) anchoring on a 3D rGO-CNT sandwich-stacked framework for highly efficient methanol and ethanol electro-oxidation, Electrochimica. 227 (2017) 330-344.

[57] J.R. Rodriguez, S. Fuentes-Moyado, T.A. Zepeda, J.N. Díaz de León, J. Cruz-Reyes, M.T. Oropeza-Guzman, G. Berhault, G. Alonso-Núñez. Methanol electro-oxidation with alloy nanoparticles of Pt10x–Fex supported on CNTs, Fuel. 182 (2016) 1–7.

[58] Chen, W., Zhang, Y. & Zhu, Z. Effects of Cerium Oxides on the Catalytic Performance of Pd/CNT for Methanol Oxidation, Chem. Res. Chin. Univ. 35 (2019) 133–138.

[59] Surin Saipanya, Somchai Lapanantnoppakhun, Thapanee Sarakonsri. Electrochemical Deposition of Platinum and Palladium on Gold Nanoparticles Loaded Carbon Nanotube Support for Oxidation Reactions in Fuel Cell, J. Chem. (2014). doi.org/10.1155/2014/104514

[60] W. Xiuyu, Z. Jingchang, Z. Hong. Pt-Au/CNT@TiO2 as a High-Performance Anode Catalyst for Direct Methanol Fuel Cells, Chinese J. Catalysis 32 (2011) 74–79.

# SUPPLEMENTARY MATERIAL

## Dye diazonium-modified carbon nanotubes with immobilized gold nanoparticles as nanohybrid electrocatalyst of direct methanol oxidation

Asma Bensghaïer[1*], Viplove Bhullar[2], Navdeep Kaur[2], Momath Lo[3], Myriam Bdiri[1]
Aman Mahajan[2*], Mohamed M. Chehimi[1]*

[1] Université Paris Est, ICMPE (UMR7182), CNRS, UPEC, F-94320 Thiais, France
[2] Department of Physics, Guru Nanak Dev University, Amritsar-143005, Punjab, India
[3] Université Cheikh Anta Diop, Faculté des Sciences, BP 5005 Dakar-Fann, Senegal

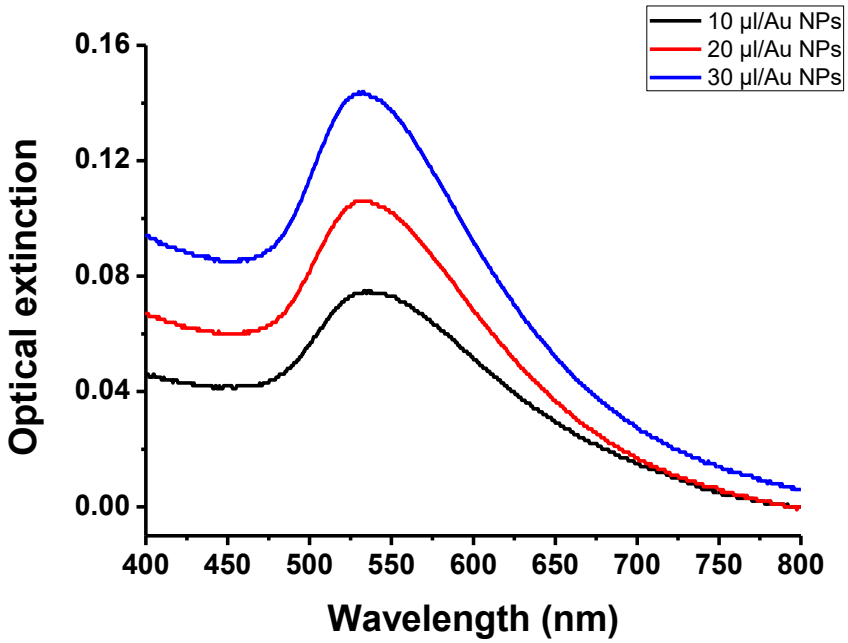


**Supplementary Material SM1.** UV-Visible extinction spectra at three different concentrations of gold colloidal suspensions prepared under the same conditions from (10-30 µl of Au NPs solution).

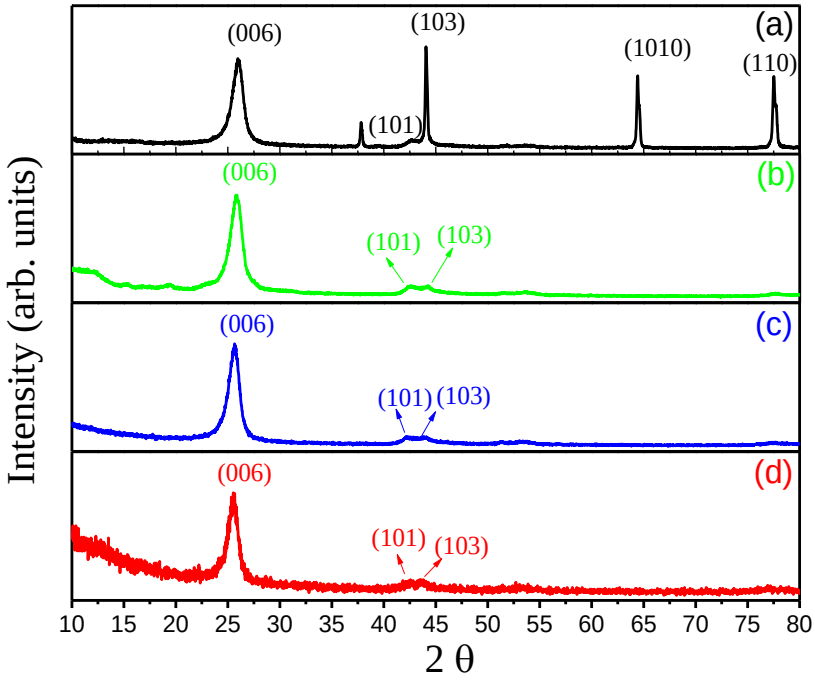


**Supplementary Material SM2** (a) XRD pattern of (a) CNT, (b) CNT-CR, (c) CNT-NR, (d) CNT-AA. Diffraction peaks are indexed as C (JCPDS file no. 26-1076)

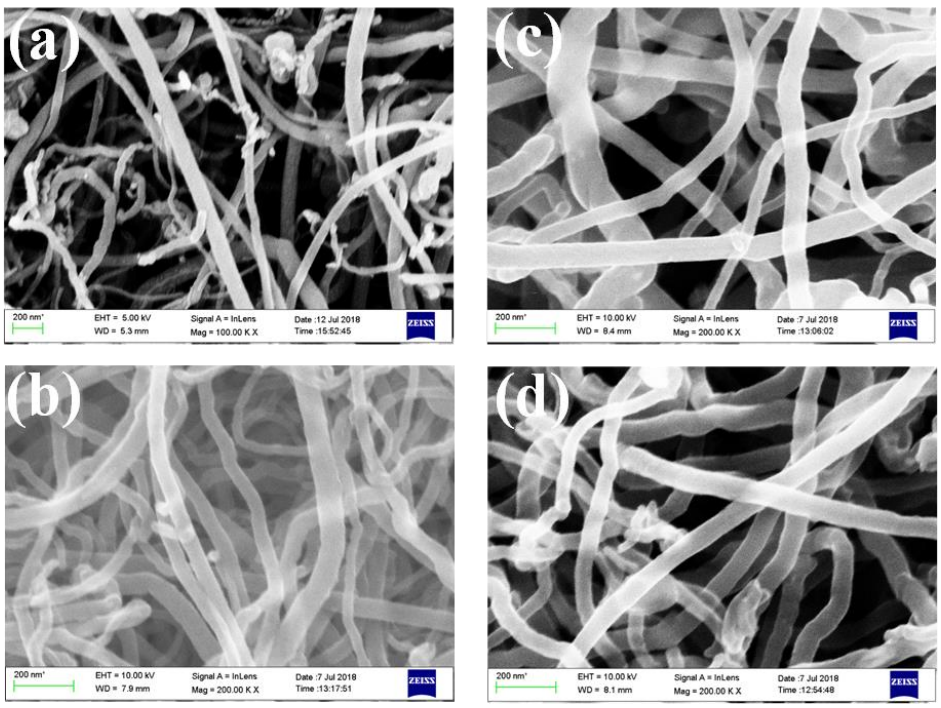

**Supplementary Material SM3.** SEM images of MWCNT (a), CNT-AA (b), CNT-NR (c) and CNT-CR (d).

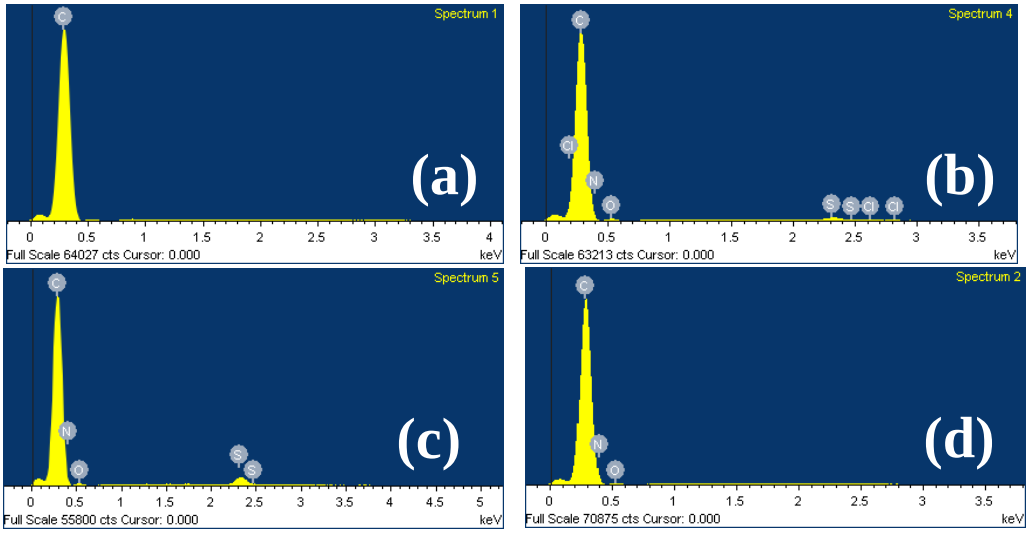


**Supplementary Material SM4.** EDX spectrum of CNT (a), CNT-AA (b), CNT-CR (c), and CNT-NR (d).

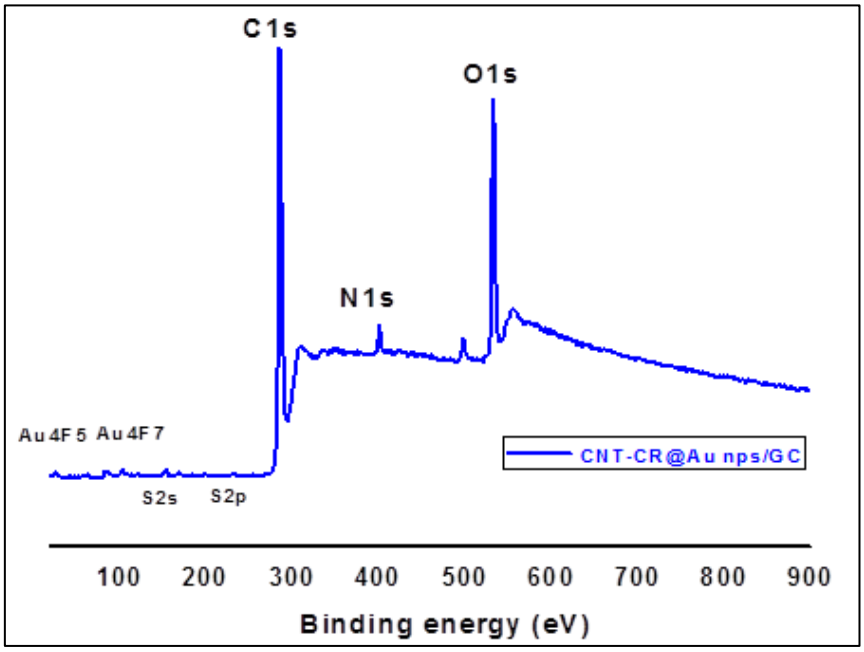


**Supplementary Material SM5:** XPS survey region of CNT-CR@Au NPs